CHAPTER 3

ADSORPTION STUDIES OF ANIONIC DYES WITH PALM SHELL CARBON

3.1 Introduction

More than 50% of the world production of dyes consists of azo dyes [3.1]. They are aromatic compounds including one or more azo groups (–N=N–) and may also contain sulfonate groups [3.2, 3.3]. It is estimated that annually 280,000 t of textile dyes are discharged in such industrial effluent, out of that azo dyes make up about a half of all known dyestuffs in the world, making them the largest group of synthetic colorants released into the environment [3.4]. Azo dyes are extensively used in textile dyeing due to their superior fastness to the applied fabric, high photolytic stability, and their resistance to microbial degradation. However, acid dyes exhibit low levels of fixation with the fiber and up to 10–50% of total dye used in dyeing process remain left in the spent dye bath [3.5]. Improper discharge of these coloured effluents in aqueous ecosystems is highly visible and affects the aesthetic merit, water transparency, and gas solubility in lakes, rivers, and other water bodies and depicts acute toxic effects on aquatic flora and fauna. Moreover, coloured effluents inhibit germination of several plants having important ecological roles, by decreasing soil fertility [3.6, 3.7]. In addition, humans can be exposed to azo dyes through water consumption or skin contact, and active metabolites can be generated in exposed cells either through the action of microorganisms in the intestinal flora [3.8] or due to bacterial activities in human skin [3.9]. Basically, cytotoxicity of typical azo dyes may be relatively low, but the toxicity of related aromatic amine intermediates is likely to be significantly high due to their carcinogenicity and/or mutagenicity [3.10-3.12]. Azo dyes cannot be easily removed by conventional treatment processes due to their stability under light, heat, oxidizing agents and biological degradation. In the degradative conditions cleavage of azo linkages in their structure also can produce toxic aromatic amines. These derived compounds can exhibit more toxic effects to the environment than the parent compound [3.13]. Therefore, the effective treatment of dye contaminated effluents is currently a primary environmental concern.

Among azo dyes, three anionic dyes -acid violet 7 (AV7), acid orange II (AO II) and disulfine blue (DSB) have been used as model dyes in this study.

Preliminary investigations done to study the removal of anionic dyes -acid orange II, acid violet-7 and disulphine blue using palm shell powder revealed that removal was only 41.961, 29.351 and 22.866% respectively. In this work, we have investigated further, ability of APSP to remove acidic anionic dyes like acid orange II, acid violet-7 and disulphine blue. The kinetic and equilibrium data of adsorption studies were processed to understand the adsorption mechanism of the dye molecules onto the acid treated palm shell powder (APSP).

Structures of dyes

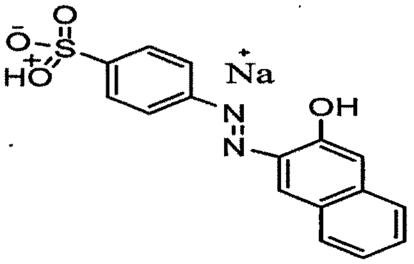

Acid Orange II

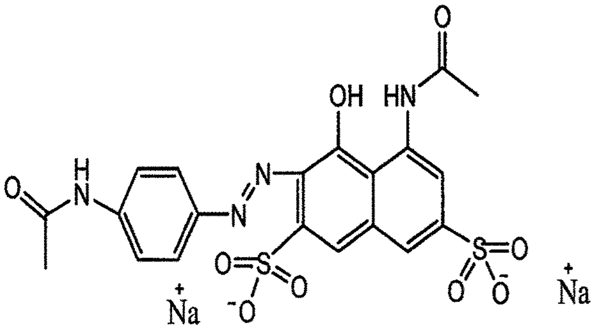

Acid Violet 7

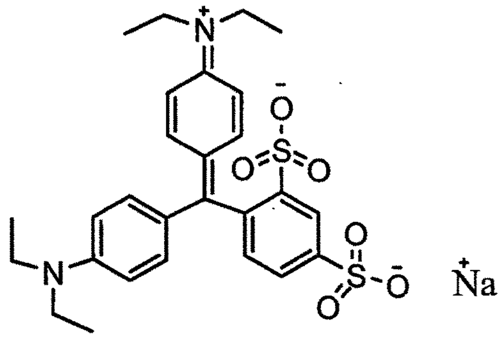

Di Sulphine Blue

3.2 Preparation of Adsorbent:

Palm shells obtained from the coastal areas of Andhra Pradesh were washed, sundried for 24 hours and ground using jaw crusher. They were then dried at 110^0C and the cleaned powder was mixed with conc. H_2SO_4 (sp. gr. 164) in 1:1.5 weight ratio and allowed to stand in an oven maintained at $140\text{-}160^0$ C for 24 h. The resulting char was thoroughly washed with water followed by 2% solution of $NaHCO_3$ until effervescence ceased and then left soaked in 2% solution of $NaHCO_3$ overnight. The acid treated palm shell powder (APSP) was then separated, washed with water until free of bicarbonate and dried at 105^0C.

3.3 Characterization of APSP:

The prepared APSP has been characterized by X-ray diffraction studies, BET, Fourier Transform Infra Red Spectroscopy and Scanning Electron Microscopy.

3.3.1 Fourier Transform Infra Red Spectroscopy:

Possible interactions of APSP and dye was studied by comparing the features of the spectra obtained from IR spectroscopy studies of dye, dye-loaded and –unloaded APSP (Figure 3.1 and Table.3.1). APSP showed a broad frequency ~3419.42 cm^{-1} which can be assigned to N-H/-OH stretching which after adsorption of dye molecule is shifted to 3424.65, 3383.76 and 3174.57 cm^{-1} for AO-II, DSB and

AV-7 dyes respectively. Peak ~1625.29cm^{-1} was assigned to N-H bond of amine or characteristics of the elongation of the aromatic –C=C- bonds which also has been shifted to 1617.62, 1608.24 and 1609cm^{-1} for AO-II, DSB and AV-7 dyes adsorbed on PSP respectively. Peak at 1378.58 which corresponds to C-N stretching is missing after adsorption of dye molecules. Peak at 1200 cm^{-1} is associated with the C-O stretching of the aromatic ring which is also shifted to a lower frequency region after adsorption of dyes.

Table 3.1: Fourier Transform Infra Red spectra of dye, dye loaded APSP, APSP

APSP	AOII	APSP-AOII	DSB	APSP-DSB	AV7	APSP-AV7	Assignment
3419.42	3433.40	3424.65	3411.48	3383.76	3425.43	3174.57	N-H & OH Stretching
1625.29	1619.55	1617.62	1627.66	1608.24	1582.66	1609.00	C=C, N-H bending
1378.58	-	-	1348.56	-	1346.68	-	C-N, stretching
-	1209.64	1200.01	1187.67	1176.38	1175.70	1175.39	C-O, stretching
-	1034.89	-	1049.66	1008.12	1035.17	-	C-O, stretching

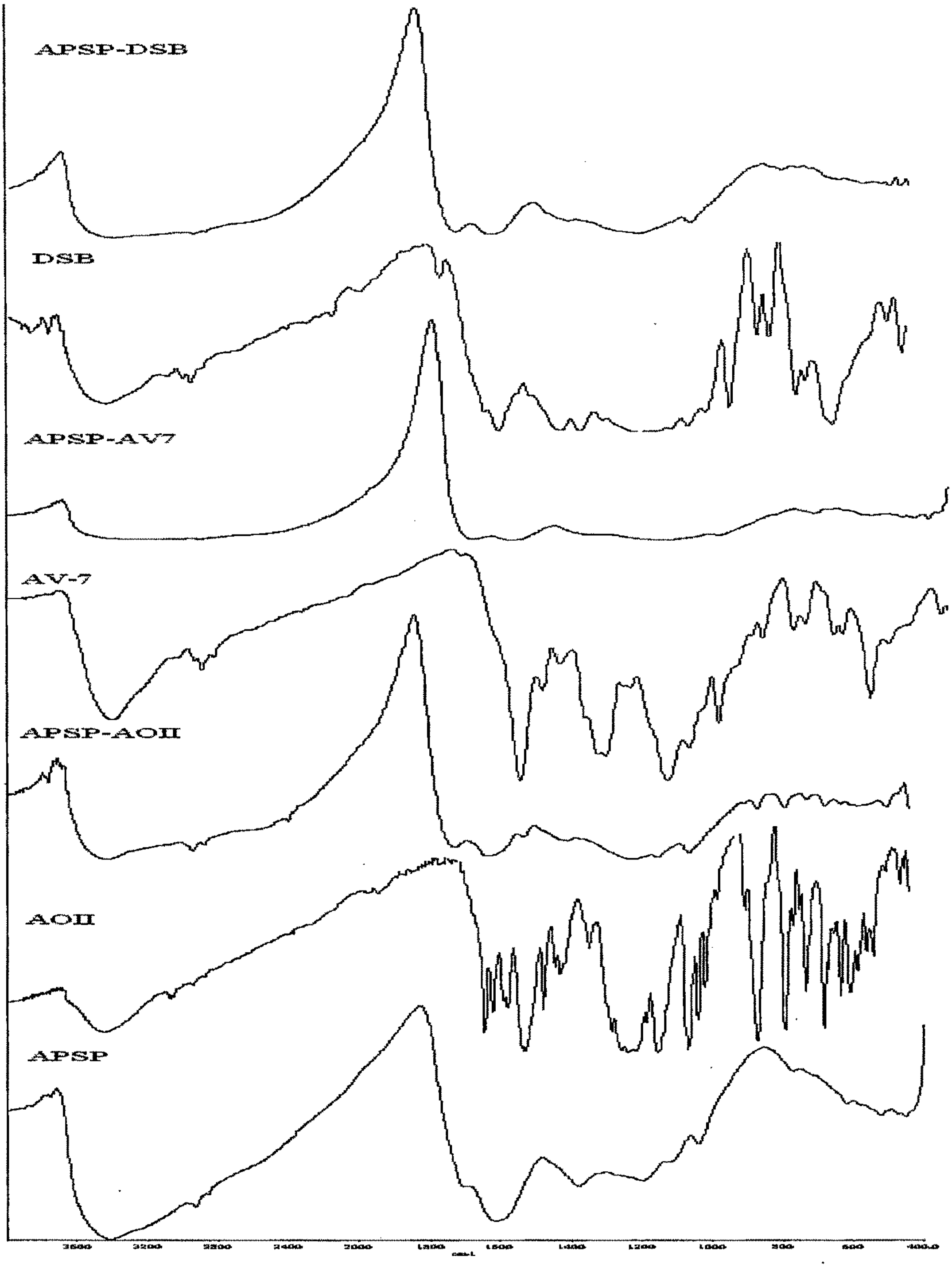

% Transmittance Vs Wave number

Figure 3.1: FTIR spectra of dye, dye loaded, unloaded APSP

3.3.2 Physical Characteristics:

The BET surface area of APSP was measured by nitrogen adsorption isotherms using BET surface area analyzer (Micrometrics ASAP 2020 V3.03 H). The BET surface area was found to be 0.2979m^2/g. The X-ray diffraction pattern of APSP (Figure 3.2) shows a peak centered around 21^0 corresponding to 002 reflection of disordered packing of micrographites. The peak is broad and suggesting amorphous structure. The peak at 21^0 corresponds to an interlayer distance of 0.423nm which suggested a disordered carbonaceous interlayer.

The morphology of APSP was studied using scanning electron microscope. The surface is magnified 1000 times (Figure 3.3) which shows that the adsorbent has an irregular rough and porous surface with identifiable micropores and mesopores.

3.4 Preparations of solutions:

All chemicals used were of analytical reagents grade.

3.4.1 Anionic dye solution 1000 ppm:

Standard 1000 ppm anionic dye solution was prepared by dissolving 1.0 g anionic dye in to 1000 mL distilled water. Appropriate volumes of this solution were diluted to obtain working standards.

3.4.2 NaOH solution 0.1 N:

Standard NaOH solution was prepared by dissolving 4.0 g NaOH in to 1000 mL distilled water and diluted to appropriate volumes.

3.4.3 HCl solution 0.1 N:

Standard 1N HCl solution was prepared by diluting 8.84 mL concentrated HCl in 100 ml distilled water and diluted to appropriate volumes

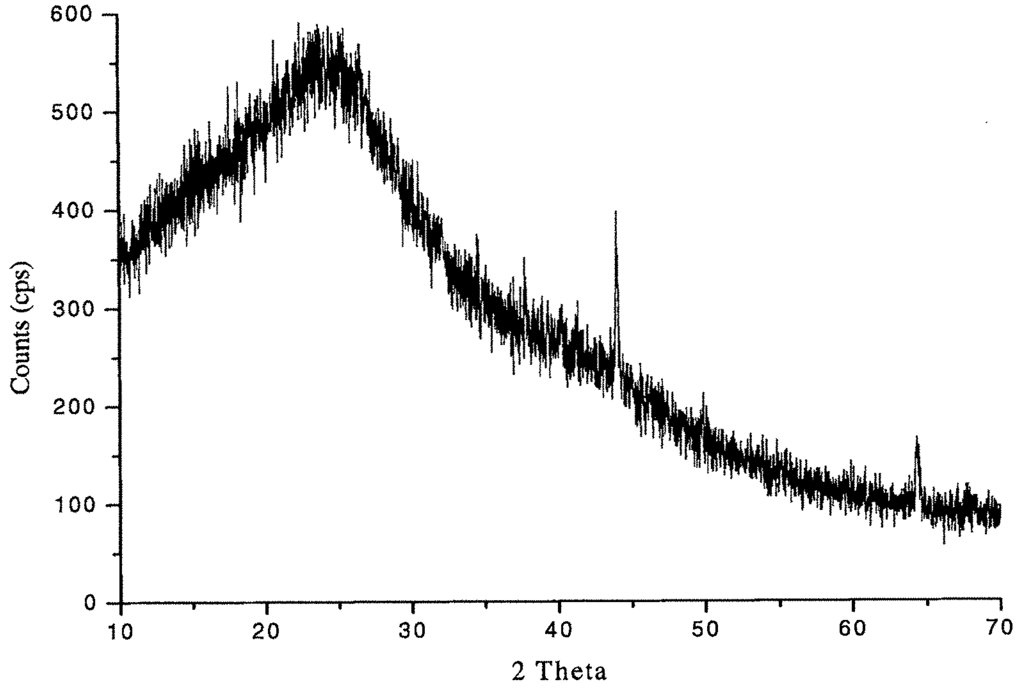

Figure 3.2: X-Ray Diffraction Study of APSP

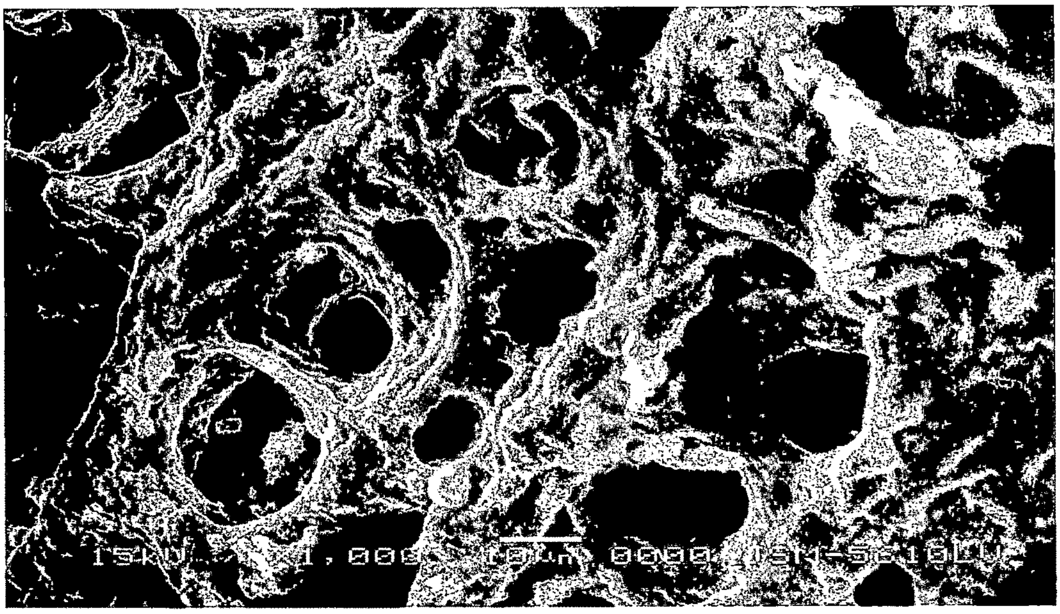

Figure 3.3: Scanning Electron Micrograph of APSP represents 1x 1,000 magnifications

3.5 Batch adsorption studies of Anionic dyes:

Adsorption studies were carried out with 100 mL Durasil Stoppered flasks containing 25 mL solution of desired sorbate concentration. A known amount of sorbent was introduced into each flask and the flasks were agitated at 180 rpm in a thermo regulated water bath shaker. A series of dye sorption experiments were conducted to study the effect of pH, dose and temperature. In the adsorption experiment a 25 mL of dye solution of known initial concentration was kept in contact with a required dose of PSP at room temperature. The pH of solutions was adjusted using 0.1N HCl or 0.1N NaOH solution using pH meter (MFRS: TOSHNIWAL INST. MFG. PVT. LTD. AJMER, CAT. NO. CL54). After a specific time period the reaction mixture was filtered. The dye concentration in the filtrate was determined by measuring absorbance at the wavelength of maximum absorption (490nm, 640nm and 530nm for AOII, DSB and AV7 respectively) using a SYSTRONICS Digital 166 model visible spectrophotometer.

The percentage removal of the dye and the amount adsorbed (mg/g) were calculated by the following relationship:

$q_e = (C_i - C_e)/m;$

Where, C_i-initial concentration of dye in mg/L; C_e – Equilibrium concentration of dye in mg/L; m – Mass of adsorbent g/L; q_e – Amount of dye adsorbed per gram of adsorbent. The experiments done without adsorbent were treated as blanks and they showed that no precipitation of dye occurred under the conditions selected.

3.6 Analysis:

The removal of the dyes was determined Spectrophotometrically (SYSTRONICS Digital Spectrophotometer 166) by measuring the absorbance values of the dye before and after treatment at their respective wavelength of maximum absorption [3.14]. The wavelengths at which calibration graphs were prepared were 640 nm for Disulphine blue and 490 nm for Acid Orange II and 530 nm for Acid Violet 7

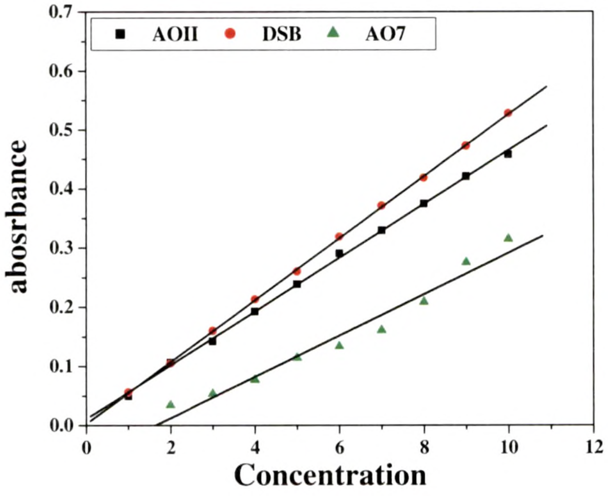

Figure 3.4: Calibration graph of AOII and DSB

3.7 Optimization parameters for adsorption of Anionic Dyes:

3.7.1 Effect of Temperature on adsorption of Dyes:

The temperature effect on the adsorption of AOII, DSB and AV7 was conducted by taking 160ppm of the respective dye in aqueous phase of volume 25mL maintained at pH-1 and equilibrating for 120 min with an adsorbent dose of 0.2g of APSP after maintaining the temperature of the solutions in the range 30-70^{0}C.

Table 3.2: Percentage uptake of dyes on APSP

Initial Concentration: 160 ppm, adsorbent: APSP, adsorbate: DSB, AOII and AV7, Volume of aqueous phase: 25 mL, Contact time: 120 min, Temperature: 30-70^{0}C, pH: 1, adsorbent Dose: 0.2 g

Temperature(°C)	**Percentage uptake of anionic dyes**		
	DSB	**AOII**	**AV7**
30	93.8000	94.4490	78.8869
40	96.0335	95.0490	78.2023
50	97.5335	95.5990	71.0247
60	97.7335	95.8740	75.3534
70	97.8335	96.2410	62.5221

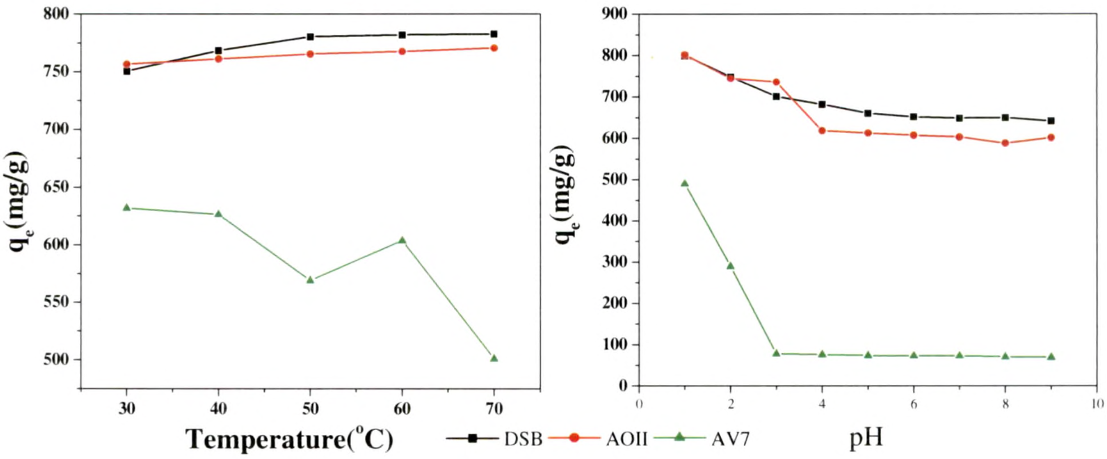

Figure 3.5: Variation in temperature and pH on adsorption of anionic dyes

Figure.3.5 and the Table 3.2 show that the adsorption of AOII and DSB increases with increasing temperature while adsorption of AV7 decreases with increasing temperature suggesting endothermic adsorption of AOII, DSB and exothermic adsorption of AV7. Increase in adsorption capacities of the dyes AOII, DSB with increasing temperature could be attributed to the increased mobility of the dye molecules with temperature and is an indication of chemisorption mechanism. Similar observations have been reported by Thangamani et al for adsorption of basic and reactive dyes [3.15]. The increase in dye adsorption with increasing temperature might also be due to the enhanced rate of intra-particle diffusion of the adsorbate as diffusion is an endothermic process [3.16].

3.7.2 Effect of pH on adsorption of Dyes:

In this study, the effect of solution pH on the adsorption of dyes was investigated in the range of 1-10 at ambient temperature (30^0C). An aqueous phase of 25 mL containing 160 ppm of each dye (DSB, AOII and AV7) adjusted to pH in the range 1-10 was agitated for 120 min in contact with 0.2 g of APSP.

Table 3.3: Percentage Uptake of dye at different pH values

Initial Concentration: 160 ppm, adsorbent: APSP, adsorbate: DSB, AOII and AV7, Volume of aqueous phase: 25 mL, Contact time: 120 min, Temperature: 30^0C, pH: 1-10, adsorbent Dose: 0.2 g

pH	Percentage Uptake		
	DSB	AOII	AV7
1	99.8812	99.9937	60.9524
2	93.4256	92.9002	35.9322
3	87.5909	91.7860	9.4827
4	85.2099	77.1052	9.2430
5	82.5569	76.4179	8.9740
6	81.4872	75.7282	8.9340
7	81.0752	75.1849	8.8980
8	81.2448	73.3384	8.6140
9	80.1890	75.0000	8.4030
10	78.8496	72.9146	

It is evident from Figure 3.5 and Table 3.3 that adsorption of all the three dyes decreases with an increase in solution pH upto ~4 and then the amount adsorbed remained almost same upto pH 10. At low pH, the positive charge on the adsorbent's surface increases which increases the electrostatic attraction between the negatively charged sulfonate anion of the dyes and the positively charged surface. But at alkaline pH significant adsorption of anionic dye occurred suggesting that chemisorption might also be operating.

3.7.3 Effect of Dose on adsorption of Dyes:

In the study, the variation in the dose of adsorbent APSP on the adsorption of dyes was conducted by agitating 160 ppm of respective dyes solution maintained at a temperature of 30^{0}C, pH-1 with different doses of adsorbent in the range 0.1-0.6g for 120 min. Figure 3.6 and Table 3.4 reveal that as the dose of the adsorbent increased from 0.1 to 0.6 g the percent adsorbed increased which can be attributed to the increase in adsorbent surface area and availability of more adsorption sites.

Table 3.4: Percentage Uptake of dyes at dose variation

Initial Concentration: 160 ppm, adsorbent: APSP, adsorbate: DSB, AOII and AV7, Volume of aqueous phase: 25 mL, Contact time: 120 min, Temperature: 30^{0}C, pH: 1, adsorbent Dose: 0.1-1.0 g

Dose (grams)	Percentage Uptake		
	DSB	**AOII**	**AV7**
0.1	37.3814	52.1277	
0.2	62.9980	78.4574	79.4613
0.3	74.1935	81.3829	80.1000
0.4	80.0759	81.3829	81.4488
0.6	86.1480	84.3085	83.2154
0.8	88.6148	85.9043	85.4019
1.0	89.1847	88.8298	86.9258

3.7.4 Effect of Agitation time:

The effect of agitation time on the adsorption of the AOII, AV7 and DSB dyes was conducted by agitating for different time intervals (10-180 min), 160 ppm of respective dye solution in a total aqueous phase volume of 25mL maintained at pH-1 and at 30 °C temperature in contact with 0.2 g APSP. The effect of agitation time on the amount adsorbed of the three dyes is shown in Figure 3.6 and Table 3.5. It was observed that as the agitation time increases from 10 minutes to 60 minutes the adsorbed amount also increased. But the equilibrium was achieved within 30min in the case of all the three dyes. The curves were smooth and continuous. Similar results were reported for various dye adsorptions using other adsorbents [3.15-3.18]. Equilibrium time is reported to be one of the important consideration for water treatment system and hence economics of the treatment system [3.19].

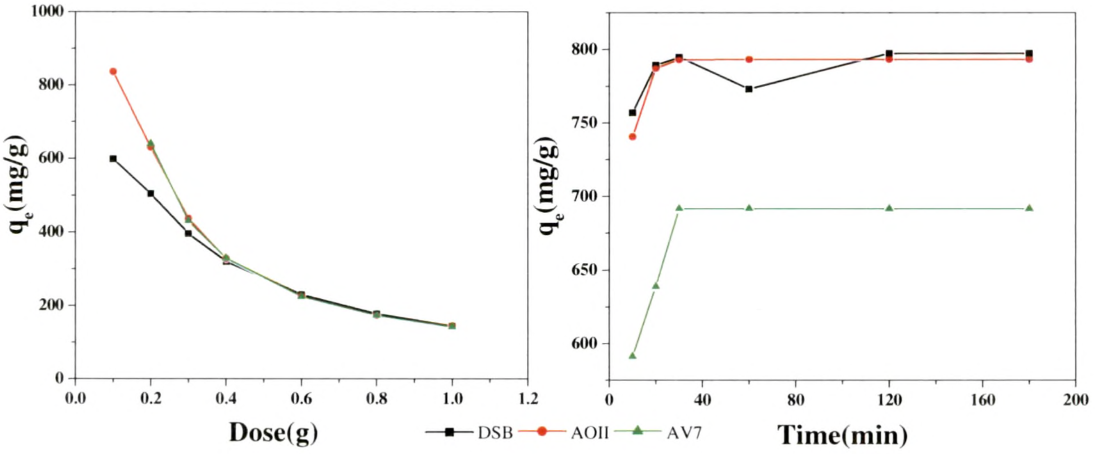

Figure 3.6: Variation in dose and Time on adsorption of anionic dyes

Table 3.5: Percentage Uptake dye with time variation

Initial Concentration: 160 ppm, adsorbent: APSP, adsorbate: DSB, AOII and AV7, Volume of aqueous phase: 25 mL, Contact time: 10-180 min, Temperature: 30^{0}C, pH: 1, adsorbent Dose: 0.2 g

Time(min)	Percentage Uptake		
	DSB	AOII	AV7
10	94.6000	92.4817	73.8074
20	98.6667	98.3191	79.7482
30	99.3333	99.0526	86.3737
60	96.6333	99.0831	86.3700
120	99.6667	99.0831	86.3516
180	99.6667	99.0831	86.3500

3.7.5 Effect of concentration on adsorption of Anionic dyes:

The effects of initial concentration of DSB and AOII on the amount of dye adsorbed on APSP were studied to obtain the adsorption capacity. Different concentrations of the respective dyes ranging from 40–400 ppm in a total aqueous phase volume of 25 mL, with the pH of the medium maintained 1 was agitated with 0.2g of APSP for 60 min and the amounts adsorbed on respective adsorbent were determined as described earlier was observed that adsorption of dye decreased with an increase in dye concentration in the solution, suggesting that removal of dye is dependent upon the concentration of the dye solution. But as a whole the q_e value increased with the increase in dye concentration as observed in the plot in Figure 3.7 From Table 3.6 it was observed that as the concentration of dye increased the percentage removal decreased indicating that the number of adsorption sites on the adsorbent decreases by increasing adsorbate concentration.

Table 3.6: Variation in the concentration of anionic dyes adsorption on APSP

Concentration: (40-400) ppm, adsorbate: APSP, pH: 1, agitation time: 60 min, dose: 0.2g, volume: 25 mL, Temperature: 40°C, adsorbent: DSB, AOII

Concentration (ppm)	Percentage Uptake	
	DSB	AOII
40	99.4000	99.6027
80	99.3667	98.4413
160	98.7500	94.8349
240	93.0000	88.4169
320	77.1667	74.6638
400	74.5330	64.8533

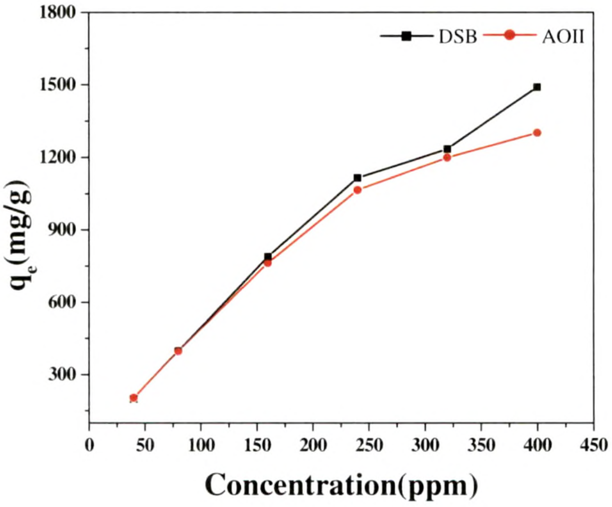

Figure 3.7: Variation in concentration of anionic dyes

3.7.6 Adsorption Isotherms:

Linear plots of log(x/m) Vs log C_e (Figure 3.8) shows that adsorption follows Freundlich isotherm model. The values of 1/n, less than unity is an indication that significant adsorption takes place at low concentration but the increase in the amount adsorbed with concentration becomes less significant at higher concentration and vice versa [3.20-3.22]. The magnitude of K_F and n shows easy removal of dye and high adsorption capacity. Table 3.7 and Figure 3.8 shows the values of the parameters of the two isotherms and the related correlation coefficients. As seen from Table.3.6, the Langmuir model and Freundlich model have good correlation values. As also illustrated in Table 3.7, the value of $1/n$ is -1.7576(AOII) calculated from the slope of the plot of Freundlich isotherm which indicates favourable adsorption [3.23]. Conformation of experimental data to Langmuir isotherm model indicates the homogenous nature of APSP surface and monolayer coverage of dye molecules at the outer surface of the adsorbent. Similar observation was reported for the adsorption of acid orange onto activated carbon prepared from agricultural waste baggasse [3.24], adsorption of direct dyes onto activated carbon prepared from sawdust [3.25] and adsorption of congo red dye on activated carbon from coir pith [3.20]. Table 3.8 shows the comparison of maximum monolayer adsorption capacity of some dyes on various adsorbents reported in literature with acid treated PSP used in this work. It is evident that the adsorbent used in this work has higher adsorption capacity as compared to those cited in literature. The adsorption capacity of APSP used in present studies was 2180.05mg/g, 1199.99mg/g and 243.9mg/g for AOII, DSB and AV7 respectively.

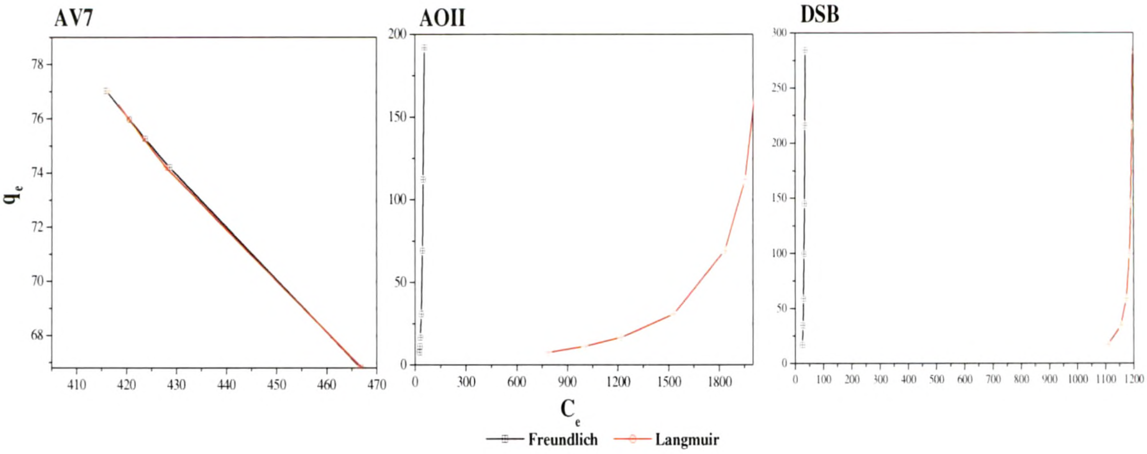

Figure 3.8: Isotherms for DSB, AOII and AV7

Table 3.7: Isotherm Parameters for DSB, AOII and AV7

Initial Concentration: 160 ppm, adsorbent: APSP, adsorbate: DSB, AOII and AV7, Volume of aqueous phase: 25 mL, Contact time: 60 min, Temperature: 30-70^{0}C, pH: 1, adsorbent Dose: 0.2 g

Isotherms	Parameter	AV7	AOII	DSB
Freundlich	K_f (mg/g)(dm^3/mg)$^{1/n}$	13898.6	16.6648	16.7535
	N	-1.2380	4.4256	7.5665
	r^2	0.9990	0.9930	0.9980
Experimental	q_e (mg/g)	415.9	2039.59	1193.991
Langmuir	q_m (mg/g)	243.9	2180.05	1199.988
	K_a (L/mg)	-0.0313	0.0757	0.7003
	r^2	0.999	0.997	0.998

Table 3.8: Comparison of maximum adsorption capacities of dyes

Material	Dye	mg/g	References
Maize cob	Acid Blue 25	41.4	[3.26]
Baggase pith	Acid Blue 25	20-25	[3.33]
Wood shavings	Congo Red	0.8	[3.32]
Sunflower stalks	Congo Red	31.5-37	[3.31]
Coir pith carbon	Congo Red	6.7	[3.20]
Sludge based activated carbon	Acid Brown 283	20.5	[3.27]
Chemviron GW activated carbon	Acid Brown 283	18.7	[3.27]
Banana pith	Acid brilliant blue	4.4	[3.28]
Kapok fruit shell	Acid Violet	1.780	[3.29]
Cashew nut shell carbon (CC)	Acid Violet	1.975	[3.29]
APSP	AOII	2180.05	Present study
APSP	AV7	243.9	Present study
APSP	DSB	1199.988	Present study

3.7.7 Adsorption Dynamics:

To study the adsorption kinetics, pseudo first order, pseudo second order and intra-particle diffusion models were checked (Figure 3.9) and calculated rate constants and r^2 values are given in Table 3.9. It is seen that the correlation coefficient was found to be 0.987 in pseudo first order model and q_e experimental values are comparatively closer with q_e theoretical than pseudo second order model but with minor deviations suggesting that pseudo first order is not a good fit. As seen from Figure 3.8, though the pseudo-second order equation better describes the adsorption process with a correlation coefficient of 0.99, the q_e experimental values are not at all comparable with q_e theoretical.

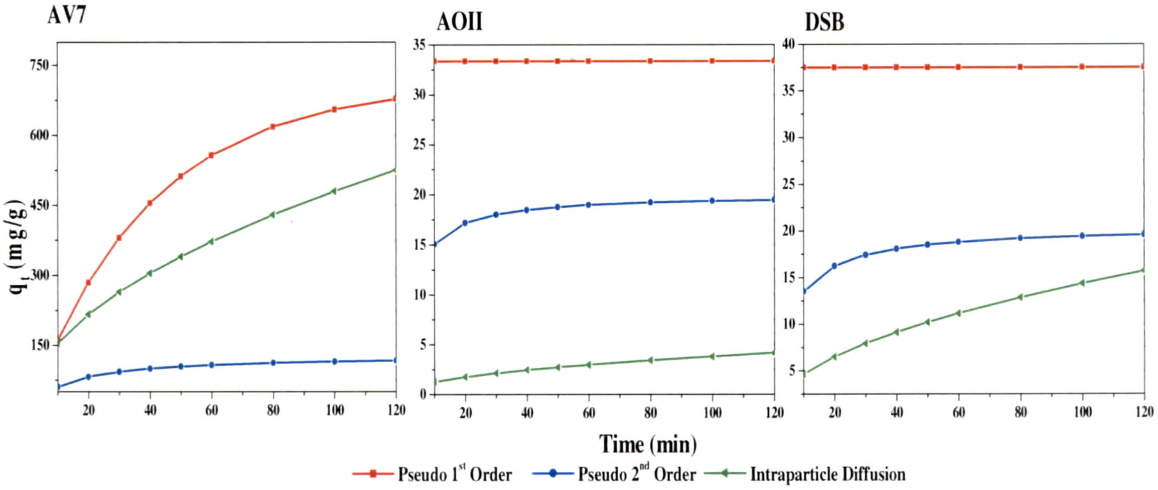

Figure 3.9: Kinetics for DSB, AOII and AV7

Table 3.9: Kinetics Parameters for DSB, AOII and AV7

Initial Concentration: 160 ppm, adsorbent: APSP, adsorbate: DSB, AOII and AV7, Volume of aqueous phase: 25 mL, Contact time: 10-120 min, Temperature: 30^{0}C, pH: 1, adsorbent Dose: 0.2 g

Kinetics	Parameter	AV7	AOII	DSB
Experimental	q_e (mg/g)	655.1200	48.4080	35.3500
Pseudo 1st Order	q_e (mg/g)	709.4100	33.2670	37.4300
	K (min^{-1})	0.0254	0.9667	0.9014
	r^2	0.9420	0.9870	0.9430
Pseudo 2nd Order	q_e (mg/g)	125.6281	19.8925	20.3087
	K (g/mg min)	0.0007	0.0151	0.0095
	r^2	0.9930	0.9990	0.9985
Intra-particle Diffusion	K_i(mg/gmin$^{0.5}$)	47.7400	0.36763	1.4226
	r^2	0.994	0.90281	0.93514

Study of intra-particle diffusion model gave r^2 values of greater than ~0.91 and plot between adsorbate concentration and square root of time was linear suggesting that adsorption process could be controlled by intra-particle diffusion. The adsorption at higher temperatures becomes more dependent on intra-particle diffusion, which would be the rate determining step.

3.7.8 Thermodynamic Parameters:

The thermodynamic parameters such as change in free energy (ΔG^o), enthalpy (ΔH^o) and entropy (ΔS^o) obtained for the adsorption of dyes under investigation are given in Table 3.10. Also negative values for the entropy for AOII and DSB shows a high affinity of PSC for AOII, DSB; furthermore the negative values of free energy and enthalpy indicate the feasibility and spontaneous values of the process. The structures of the dye molecules may be an important factor for their adsorption.

The negative values of ΔG^o confirm that the dye adsorption on APSP is a spontaneous process. It has been reported that ΔG^o up to -20 kJ/mol are due to electrostatic interaction between adsorption sites and the adsorbate (physical adsorption), while ΔG^o values more negative than -40 kJ/mol involve charge sharing or charge transfer from the biomass surface to the adsorbate to form a coordinate bond [3.34]. The ΔG^o values obtained in this study for the two dyes are <-10 KJ/mol, which indicates that physical adsorption was the predominant mechanism in the adsorption process.

Table 3.10: Thermodynamic Parameters for DSB and AOII

Initial Concentration: 160 ppm, adsorbent: APSP, adsorbate: DSB and AOII, Volume of aqueous phase: 25 mL, Contact time: 5-60 min, Temperature: 30-70^{0}C, pH: 1, adsorbent Dose: 0.2 g

Time (min)	Temp (K)	ln K		-ΔG° KJ/ mole		ΔS° KJ/ mole		ΔH° KJ/ mole	
		DSB	AOII	DSB	AOII	DSB	AOII	DSB	AOII
60	303	1.3303	1.4573	3.3513	3.6712	-0.0669	-0.0163	23.6207	8.6204
	313	1.8005	1.5685	4.6854	4.0817	-0.0021	-0.0143	5.3389	8.5653
	323	2.2910	1.692	6.1524	4.5438	0.0001	-0.0094	6.1140	7.5689
	333	2.3777	1.7595	6.5827	4.8712	0.0066	-0.0130	4.3822	9.2033
30	303	0.3509	0.6582	0.8840	1.6581	-0.1104	-0.0363	34.3355	12.6465
	313	1.0975	1.0023	2.856	2.6083	-0.0710	-0.0146	25.0775	7.1798
	323	1.5794	1.055	4.5414	2.8331	-0.0383	-0.0181	16.6267	8.6856
	333	1.6766	1.1728	4.6418	3.2470	-0.0613	-0.0105	25.0561	6.7304
20	303	0.2231	0.3991	0.5621	1.0053	-0.0878	-0.0242	27.2260	8.3313
	313	0.5295	0.6432	1.3778	1.6739	-0.0863	-0.0081	28.3859	4.2101
	323	1.0515	0.7167	2.8238	1.9247	-0.0529	-0.0037	19.8953	3.1298
	333	1.3891	0.7326	3.8459	2.0282	-0.0154	-0.0088	8.9617	4.9489
10	303	-0.9669	-0.3863	-2.4358	-0.9731	-0.1375	-0.0557	39.2167	15.9155
	313	-0.3403	-0.1386	-0.8856	-0.3607	0.3149	-0.0476	97.6928	14.5510
	323	0.3827	-0.0849	1.0277	-0.2280	0.0632	-0.0628	21.4532	20.0483
	333	0.6708	0.1135	1.8572	0.3142	0.0563	-0.0563	16.8738	22.4951
5	303	-1.1044	-0.8663	-2.7821	-2.1823	-0.0846	-0.0709	22.8380	19.313
	313	-0.8541	-0.6451	-2.2226	-1.6787	-0.0838	-0.0693	24.0052	20.0195
	323	-0.5193	-0.4325	-1.3945	-1.1614	-0.0717	-0.0692	21.7456	21.1953
	333	-0.0745	0.0123	-0.2063	0.0340	-0.0084	-0.0043	2.5935	1.4688

3.7.9 Adsorption Mechanism:

pH studies and Langmuir isotherms are indicative of two mechanisms operating for adsorption of anionic dyes on APSP. They include electrostatic attraction between the protonated adsorbents and acidic dyes and the chemical reaction between the adsorbate and the adsorbent system. Conformation to Langmuir isotherms also indicates the homogenous nature of APSP surface suggesting each dye molecule/acid treated PSP adsorption has equal adsorption activation energy and monolayer coverage of dyes [3.35]. Conformation to pseudo second order model suggests that the rate determining step may be chemisorption involving valency forces through sharing or exchange of electrons between adsorbent and adsorbate. The endothermic nature of adsorption of AOII and DSB suggests that intra-particle diffusion also plays a significant role in the adsorption process of these dyes.

Netrapadit et al. stated that a lower amount of sulphonic groups (SO_3^-) decreases the amount negative charge and attractive force with positive charges [3.36]. Though AOII has lower number of SO_3^- has greatest adsorption capacity followed by DSB and AV7 probably due to geometry and size of the molecule. AV7 could be more protonated at pH-1 than DSB and hence adsorption of DSB is more compared to AV7 because of electrostatic repulsion of AV7 with the adsorbent surface. Moreover since chemisorption is also operating the trend can not be explained on the basis of electrostatic attraction/ repulsion alone.

Based on the results obtained from the IR analysis and pH, kinetic and the isotherm studies, we conclude that the adsorption mechanism, underlying the adsorption of dyes onto APSP, might be partly ion exchange, chemisorption, physisorption and intra-particle diffusion.

3.7.10 Banghams equation:

The double logarithmic plot according to Bangham equation yielded non-linear curves showing that the diffusion of the adsorbate into the pores of the sorbent does not perfectly control the sorption process. The non-linearity of these plots confirms the non-applicability of Banghams equation and indicated that the adsorption of anionic dyes is not pore diffusion controlled.

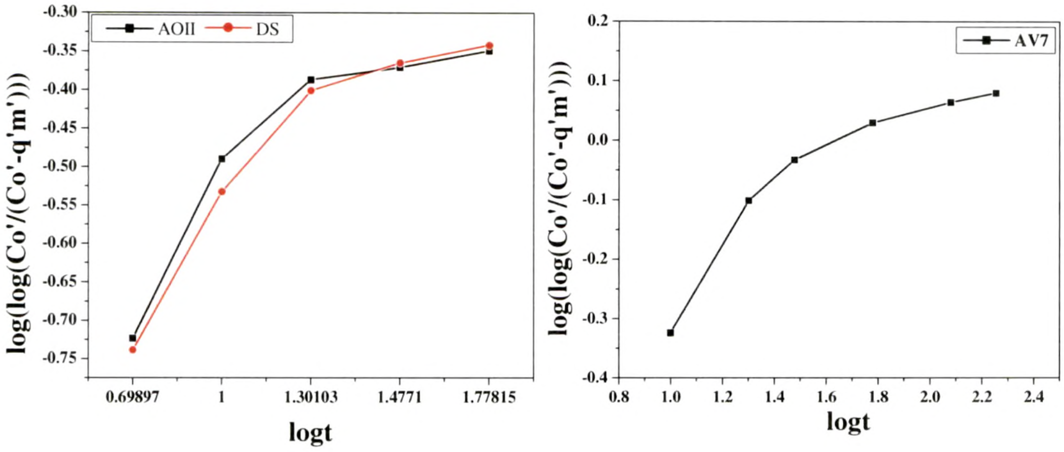

Figure 3.10: Banghams Plot of AOII, AV7 and DSB

3.8 Conclusion:

From this study it was observed that the adsorption of three anionic dyes DSB, AOII and AV 7 by low cost adsorbent APSP was convenient for the removal of anionic dyes. The results indicate that acidic pH is favorable for adsorption of anionic dye. Increasing temperature favours the adsorption of AOII and DSB dyes while lower temperature favours the adsorption of AV7 dye. Removal capacity of AOII dye was highest. Thermodynamic results indicate that the adsorption of DSB and AO II is spontaneous and endothermic while adsorption of AOII dye is exothermic. The values of maximum adsorption capacity were found to be 2180.05mg/g, 1199.99mg/g and 243.9mg/g for AOII, DSB and AV7 respectively which is comparable with the values reported in literature.

Reference:

3.1. Pandey, A., Singh, P. and Iyengar, L., "Bacterial decolorization and degradation of azo dyes", Int. Biodeter. Biodegr. 59 (2007) 73–84.

3.2. Song, Y.L., Li, J.T. and Chen, H., "Degradation of C.I. Acid Red 88 aqueous solution by combination of Fenton's reagent and ultrasound irradiation", J. Chem.Technol. Biotechnol., 84 (2009) 578–583.

3.3. Khehra, M.S., Saini, H.S., Sharma, D.K., Chadha, B.S. and Chimni, S.S., "Biodegradation of azo dye C.I. Acid Red 88 by an anoxic–aerobic sequential Bioreactor", Dyes Pigment, 70 (2006) 1–7.

3.4. Chang, J.S., Chou, C., Lin, Y., Ho, J., and Hu, T.L., "Kinetic characteristics of bacterial azo-dye decolorization by Pseudomonas luteola," Water Res., 35(2001) 2041–2050.

3.5. Kurosumi, A., Erika, K., and Nakamura, Y., "Degradation of reactive dyes by ozonation and oxalic acid-assimilating bacteria isolated from soil," Biodegradation 19 (2008) 489–494.

3.6. Wang, W, "Toxicity assessment of pretreated industrial effluent using higher plant," Res Journal Water Pollution Control Fed, 62 (1991) 853–860.

3.7. Vandevivere, P.C., Bianchi, R., and Verstraete, W., "Treatment and reuse of wastewater from the textile wet-processing industry:review of emerging technologies," J Chem Technol Biotechnol, 72 (1998) 289–302.

3.8. Chadwick, R.W., George, S.E., and Claxton, L.D., "Role of the gastrointestinal mucosa and microflora in the bioactivation of dietary and environmental mutagens or carcinogens," Drug Metabolism Rev, 24(1992) 425–492.

3.9. Stahlmann, R., Wegner, M., Riecke, K., Kruse, M., and Platzek, T., "Sensitising potential of four textile dyes and their metabolites in a modified local lymph node assay," Toxicol., 219 (2006) 113–123.

3.10. Ben Mansour H, Corroler D, Barillier D, Ghedira K, Chekir L, and Mosrati R "Evaluation of genotoxicity and pro-oxidant effect of the azo dyes: acids yellow 17, violet 7 and orange 52, and of their degradation products by Pseudomonas putida mt-2," Food Chem Toxicol 45(2007)1670–1677.

3.11. Ben Mansour H, Mosrati R, Corroler D, Ghedira K, Bariller D, Chekir L, "Genotoxic and anti-butyrylcholinesterasic activities of acid violet 7 and its biodegradation products". Drug Chem Toxicol., 32(2009) 230–237.

3.12. Ben Mansour H, Bariller D, Correler D, Ghedira K, Chekir L, and Mosrati R, "In vitro mutagenicity of acid violet 7 and its degradation products by Pseudomonas putida mt-2: Correlation with chemical structures", Environmental Toxicology and Pharmacology, 27(2) (2009) 231-236.

3.13. Hao, O.J., Kim, H.P., and Chiang, C, "Decolorization of wastewater", Crit. Rev. Environ. Sci. Technol. 30 (2000) 449–505.

3.14. Rao, K.C.L.N., Krishnaih, K., and Ashutosh., "Color Removal from a Dyestuff Industry Effluent using Activated Carbon," Indian J Chem. Tech, 1(1994) 13-19.

3.15. Thangamani, K.S., Sathish kumar, M., Sameena, Y., Vennilamani, N., Kardivelu, K., Pattabhi, S., and Yun, S.E., "Utilisation of modified silk cotton hull waste as an adsorbent for the removal of textile dye (reactive blue MR) from aqueous solution", Bioresource Technology, 98 (2007) 1265-1269.

3.16. Namasivayam, C., and Kavitha, D., "Removal of congo red from water by adsorption onto activated carbon prepared from coir pith, an agricultural solid waste", Dyes and Pigments 54 (1989) 47-58.

3.17. Sugunadevi, S.R., Sathishkumar, M., Shathi, K., Kardivelu, K. and Pattabhi, S., "Removal of direct T-blue R from aqueous solution onto carbonized sugarcane baggase waste", Indian J. Environ. Protect., 22 (2002) 500-505.

3.18. Low, K.S. and Lee, C.K. "The removal of cationic dyes using coconut husk as an adsorbent", J. Sci. Technol., 13 (1990) 221-228.

3.19. Deepa, K.K., Sathishkumar, M., Binupriya, A.R., Murugesan, G.S., Swaminathan, K. and Yun, S.E., "Sorption of Cr(VI) from dilute solutions and waste water by live and pretreated biomass of Aspergillus Flavus", Chemosphere, 62 (2006) 833-840.

3.20. Namasivayam C. and Kavitha D. "Removal of congo red from water by adsorption onto activated carbon prepared from coir pith, an agricultural solid waste", Dyes and Pigments 54 (1989) 47-58.

3.21. Haghseresht F. and Lu G., "Adsroption characteristics of phenolic compounds onto coal-reject-derived adsorbents", Energy Fuels, 12(1998) 1100-1107.

3.22. Fytianos, K., Voudrias, E. and Kokkalis, E. "Sorption-desorption behaviour of 2,4-dichlorophenol by marine sediments", Chemosphere, 40 (2000) 3-6.

3.23. Adamson, A.W., "Physical chemistry of surfaces", 5th edition, Wiley, New York, (1990).

3.24. Tsai, W.T., Chang, C.Y., Lin, M.C., Chien, S.F., Sun, H.F. and Hseih, M.F., "Adsorption of acid dye onto activated carbons prepared from agricultural waste baggase by $ZnCl_2$ activation", Chemosphere, 45 (2001) 51-58.

3.25. Mallik, P.K., "Dye removal from waste water using activated carbon developed from sawdust; adsorption equilibrium and kinetics", J. Hazard. Mater., B113 (2004) 81-88.

3.26. El-Geundi, M.S., "Color removal from textile effluents by adsorption techniques", Water Res. 25 (1991) 271.

3.27. Martin, M.J., Artola, A., Balaguer, M.D. and Rigola, M. "Activated carbons developed from surplus sewage sludge for the removal of dyes from dilute aqueous solution", Chem. Eng. J., 94 (2003) 231-239.

3.28. Namasivayam, C., Prabha, D. and Kumutha, M., "Removal of direct red and acid brilliant blue by adsorption on banana pith". Biores. Technol., 64 (1998) 77-79.

3.29. Kannan, N. and Murugavel, S., "Comparative study on the removal of acid violet by adsorption on various low cost adsorbents", Global Nest Journal, 10(3) (2008) 395-403.

3.30. El-Geundi, M.S., "Color removal from textile effluents by adsorption techniques", Water Res. 25 (1991) 271.

3.31. Sun, G. and Xu, X., "Sunflower stalks as adsorbents for color removal from textile waste water", Ind. Eng. Chem. Res., 36 (1997) 808-812.

3.32. Abo-Elila, S.I. and El-Dib, M.A., "Color removal via adsorption on wood shaving", Sci Total Environ., 66 (1987) 269-273.

3.33. McKay, G., Geundi, M. El. and Nassar, M. M., "Equilibrium studies during the removal of dyestuffs from aqueous solutions using baggase pith", Water Res., 21 (1987) 1513-1520.

3.34. Tsai, W.T., Chang, C.Y., Lai, C.W. and Lo, C.C. "Adsorption of ethyl violet dye in aqueous solution by regenerated spent bleaching earth," J. Colloid Interface Sci., (2005) 289, 333.

3.35. Gupta, V.K., Imran, A., Saini, V.K., Tom, V.G., Bart, V.D.B. and Carlo, V., "Removal of dyes from waste water using bottom ash", Ind. Eng. Chem. Res., 44 (2005) 3655-3664.

3.36. Netpradit, S., Thiravetyan, P., and Towprayoon, S., "Application of waste metal hydroxide sludge for adsorption of azo reactive dyes", Water Res., 37 (2003) 763-772.